



## Hydration process in Portland cement blended with activated coal gangue\*

Xian-ping LIU<sup>1</sup>, Pei-ming WANG<sup>1</sup>, Min-ju DING<sup>2</sup>

(<sup>1</sup>Key Laboratory of Advanced Civil Engineering Materials (Tongji University), Ministry of Education, Shanghai 201804, China)

(<sup>2</sup>State Key Laboratory Breeding Base of Crime Scene Evidence, Shanghai 200083, China)

E-mail: lxp@tongji.edu.cn; tjwpm@126.com; dingmj803@yahoo.com.cn

Received Nov. 25, 2010; Revision accepted Mar. 30, 2011; Crosschecked June 21, 2011

**Abstract:** This paper deals with the hydration of a blend of Portland cement and activated coal gangue in order to determine the relationship between the degree of hydration and compressive strength development. The hydration process was investigated by various means: isothermal calorimetry, thermal analysis, non-evaporable water measurement, and X-ray diffraction analysis. The results show that the activated coal gangue is a pozzolanic material that contributes to the hydration of the cement blend. The pozzolanic reaction occurs over a period of between 7 and 90 d, consuming portlandite and forming both crystal hydrates and ill-crystallized calcium silicate hydrates. These hydrates are similar to those found in pure Portland cement. The results show that if activated coal gangue is substituted for cement at up to 30% (w/w), it does not significantly affect the final compressive strength of the blend. A long-term compressive strength improvement can in fact be achieved by using activated coal gangue as a supplementary cementing material. The relationship between compressive strength and degree of hydration for both pure Portland cement and blended cement can be described with the same equation. However, the parameters are different since blended cement produces fewer calcium silicate hydrates than pure Portland cement at the same degree of hydration.

**Key words:** Activated coal gangue, Portland cement, Blended cement, Hydration, Strength

**doi:**10.1631/jzus.A1000479

**Document code:** A

**CLC number:** TQ172

### 1 Introduction

Coal gangue is the waste native rock excavated during coal mining, forming an industrial waste stream when coal is processed into a final product. China is the world's largest producer and consumer of coal, and coal gangue forms the majority of the country's industrial solid waste. Xie (2009) indicated that, because of continuing production, the accumulated stockpile of coal gangue reached  $4.1 \times 10^{12}$  kg in 2007. The discharge of coal gangue is increasing

every year as the coal industry expands, and is estimated to approach  $6 \times 10^{12}$  kg (Wei *et al.*, 2010). The disposal of this large quantity of solid waste requires a lot of land and causes serious environmental problems, such as heavy metal contamination in water and soil, landslides, and SO<sub>2</sub> and CO emissions into the atmosphere by spontaneous combustion. Over the last decade, with the encouragement and financial support of the government, Chinese researchers have carried out a number of studies to find productive uses for coal gangue.

The cementitious capability of fresh coal gangue is very weak (Feng, 2000), but research has shown that, after physical or chemical activation, coal gangue can react with calcium hydroxide (CH) to produce calcium silicate hydrates (C-S-H) and calcium aluminate hydrates (C-A-H), significantly improving the cementitious behavior of the material (Li *et al.*,

\* Project supported by the National Basic Research Program (973) of China (Nos. 2001CB610704 and 2009CB623104), the Youth Foundation of Key Laboratory of Advanced Civil Engineering Materials (Tongji University), Ministry of Education, China, and the Foundation of State Key Laboratory of High Performance Civil Engineering Materials (No. 2010CEM015), China

© Zhejiang University and Springer-Verlag Berlin Heidelberg 2011

2006; 2010). Therefore, a good route to minimize the environmental impact is using coal gangue as a raw material, substituting activated coal gangue (ACG) as clinker to produce blended cement, where the ACG acts as a supplementary cementing material (SCM). Research has shown that ACG-cement blends offer several advantages over pure cement, providing better properties, reducing environmental pollution, and reducing production energy and CO<sub>2</sub> emissions (Rojas and Sánchez de Rojas, 2005; Wang *et al.*, 2007; Liu and Wang, 2008; Zhang *et al.*, 2010; Wang and Liu, 2011). However, there have been few systematic studies concerning the analysis of the hydration process of ACG-cement blends during one year of curing and the relationship between the degree of hydration and the development of material properties. In this paper, we use ACG formed by high-temperature calcination with a calcium additive to prepare the blended cement, substituting 30% (w/w) of ACG for Portland cement. The hydration process and compressive strength development of blended cement were studied, and a relationship between them has been derived. This understanding of the hydration mechanisms and the connection with the mechanical characteristics of an ACG-cement blend can thus be used to optimize product properties.

## 2 Materials and methods

### 2.1 Materials

The ACG was prepared by high-temperature calcination at 820 °C for 2 h of an experimental blend of coal gangue. This blend had about 15% (w/w) calcium oxide achieved by the addition of a certain proportion of limestone. The ACG was then cooled and ground into powder. The chemical composition and particle size distribution of the ACG are given in Table 1 and Fig. 1. The density of the ACG is 2.63 g/cm<sup>3</sup>, the specific surface area is 600 m<sup>2</sup>/kg, and the free calcium oxide (f-CaO) content is 0.82%

(w/w). Some of the dried powder was ground to approximately 5 μm to apply to the phase analysis. According to an X-ray diffraction (XRD) (D/max2550VB3+/PC, RIGAKU, Japan) examination of the ACG (Fig. 2), the main minerals present are quartz (SiO<sub>2</sub>), feldspars (including anorthite (CaAl<sub>2</sub>Si<sub>2</sub>O<sub>8</sub>), gehlenite (Ca<sub>2</sub>Al<sub>2</sub>SiO<sub>7</sub>), akermanite (Ca<sub>2</sub>MgSiO<sub>7</sub>), and microcline (KAlSi<sub>3</sub>O<sub>8</sub>)), rutile (TiO<sub>2</sub>), hematite (Fe<sub>2</sub>O<sub>3</sub>), calcium oxide (CaO), and calcite (CaCO<sub>3</sub>). Gismondine and potassium calcium sulfate are also present. The diffuse hump from 20°–40° indicates the presence of some amorphous phases, and a Fourier transform infrared spectroscopy (FTIR) (Equinoxss/Hyperion2000, Bruker, Germany) examination indicates that these are silica and alumina (Fig. 3). In the FTIR spectra, the band at 563 cm<sup>-1</sup> belongs to metakaolin. The bands at 3436, 1639, 475 cm<sup>-1</sup> and the large band at 1100–1000 cm<sup>-1</sup> are attributed to amorphous silica. The bands in the 1009, 870, and 693 cm<sup>-1</sup> regions are indicative of the presence of a zeolitic precursor (an amorphous aluminosilicate network structure) in the samples. The FTIR analysis results are in accordance with results presented in the literature (Shigemoto *et al.*, 1995; Palomo *et al.*, 1999; Kakali *et al.*, 2001; Shvarzman *et al.*, 2003). The existence of metakaolin is also confirmed by the peak at  $-103 \times 10^{-6}$  (Q<sup>4</sup>(1Al)) in the <sup>29</sup>Si nuclear magnetic resonance (NMR) (AV400(SB), Bruker, Switzerland) spectra (Fig. 4a) and the peak at  $38 \times 10^{-6}$  (AlO<sub>4</sub>) in the <sup>27</sup>Al NMR spectra (Fig. 4b) of the ACG. The peaks in the <sup>29</sup>Si NMR spectra (Fig. 4a) between  $-(70-99) \times 10^{-6}$  are broad and separate. This is due to the dissymmetrical structure of Q<sup>0</sup>, Q<sup>1</sup>, Q<sup>2</sup>, and Q<sup>3</sup> having different numbers of tetrahedral Al connected via oxygen bridges to a given SiO<sub>4</sub> tetrahedron belonging to metakaolin (Lippmaa *et al.*, 1980; Singh *et al.*, 2005; Zibouche *et al.*, 2009).

Pure Portland cement (PC) was used as the control sample and the blended sample (PG) was prepared with a 30% (w/w) substitution of ACG. The chemical compositions and particle size distributions

**Table 1 Chemical compositions of ACG, PC, and PG**

Material	Chemical composition (% w/w)									
	CaO	SiO <sub>2</sub>	Al <sub>2</sub> O <sub>3</sub>	Fe <sub>2</sub> O <sub>3</sub>	MgO	K <sub>2</sub> O	SO <sub>3</sub>	Na <sub>2</sub> O	TiO <sub>2</sub>	Loss
ACG	14.63	57.00	17.70	3.33	1.56	1.99	0.41	0.46	0.60	2.02
PC	64.78	20.34	5.02	3.11	1.09	0.35	2.20	0.10	0.26	1.73
PG	47.50	33.70	7.98	2.37	0.95	0.79	2.00	0.20	0.29	1.82

of the two cements are given in Table 1 and Fig. 1. The phase composition of PC, calculated using Bogue's equations, is given in Table 2. The densities of the PC and the PG are 3.16 and 2.98 g/cm<sup>3</sup>, the specific surface areas are 370 and 440 m<sup>2</sup>/kg, and the f-CaO contents are 0.38% and 0.52% (w/w), respectively. Since the ACG is a light porous material, the 30% (w/w) addition of the ACG into PC lowers its density by approximately 6%, and increases its specific surface area by approximately 19%.

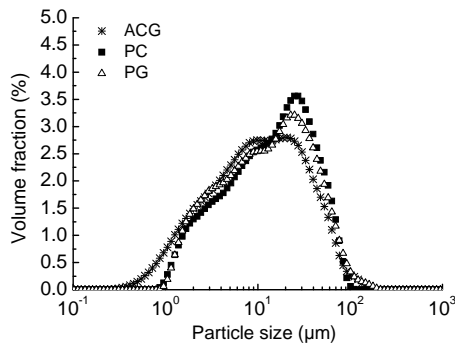


Fig. 1 Particle size distributions for activated coal gangue, Portland cement, and the blended sample

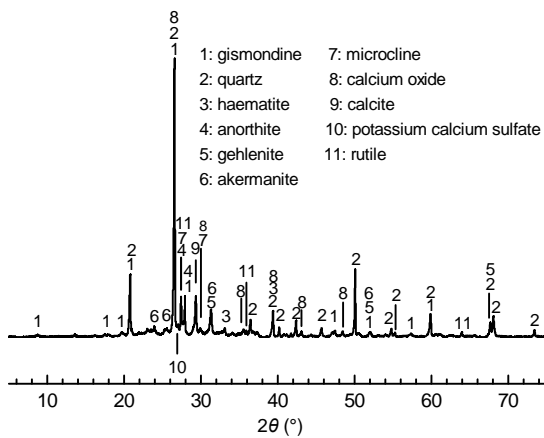


Fig. 2 X-ray diffraction results for activated coal gangue

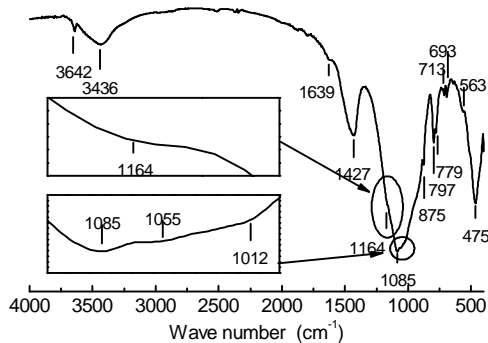


Fig. 3 Fourier transform infrared spectra for activated coal gangue

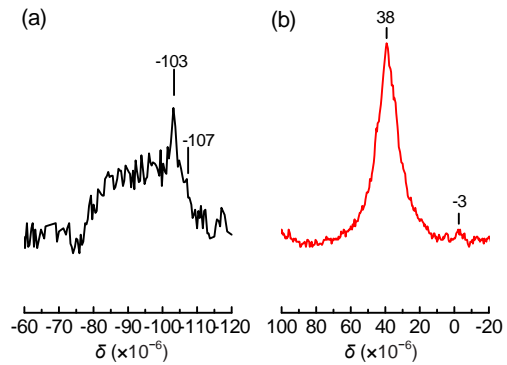


Fig. 4 <sup>29</sup>Si (a) and <sup>27</sup>Al (b) nuclear magnetic resonance spectra for activated coal gangue

Content	Composition (% w/w)	Content	Composition (% w/w)
C <sub>3</sub> S	64.60	C <sub>4</sub> AF	9.45
C <sub>2</sub> S	9.56	CaSO <sub>4</sub>	3.74
C <sub>3</sub> A	8.05		

## 2.2 Methods

The pozzolanic activity of the ACG was correlated with the existence of CH and gypsum under the same water binder ratios and curing conditions as those of the cement pastes. A total of 6 g of ACG was added to 3.21 g of tap water, followed by the addition of 4 g of CH and 0.7 g of gypsum. Then 20 mm cube samples of the mixture were prepared using steel molds and cured at (20±3) °C at a relative humidity ≥ 95%. The samples were removed from the molds after 1 d and then cured for controlled durations in an airtight sealed container at 20 °C. The amount of CH remaining after the pozzolanic reaction at 1, 3, 7, 28, 90, and 360 d was determined using differential scanning calorimetry (DSC) (Fig. 5).

The PC and PG pastes were prepared with a water binder ratio of 0.3. The heat evolved during the reaction was determined by means of an isothermal calorimeter. The 20 mm cube samples were cast in steel molds and cured at (20±3) °C with relative humidities maintained ≥95%. The samples were removed from the molds after 1 d and cured in airtight sealed containers at 20 °C. The compressive strength of cubic samples was determined at 1, 3, 7, 14, 28, 56, 90, 180, and 360 d. The fractured pieces (nominal size of 10 mm) obtained from the compressive strength test were subjected to drying treatment, first with ethanol and then in a vacuum oven at 45 °C for 24 h to stop the hydration reaction. To determine the CH

content with DSC, the degree of hydration by the non-evaporable water method, and to determine the variety of hydrates present by XRD, the dried pieces were then ground to pass through an 80  $\mu\text{m}$  sieve.

Fully hydrated PC and PG samples were prepared to determine the degree of hydration of the cement pastes after different reaction times using the non-evaporable water method. After the PC and PG pastes were made with a water binder ratio of 0.3, they were cured in airtight sealed containers at 20  $^{\circ}\text{C}$  for 1 d, and then ground by ball mill to a mean particle diameter of about 45  $\mu\text{m}$ . Then the powders were mixed with water at a water powder ratio of 0.3 and cured in airtight sealed containers at 20  $^{\circ}\text{C}$ . During the curing period, samples from 3, 7, and 28 d cure times were ground by ball mill to a mean particle diameter of about 10  $\mu\text{m}$ . After 360 d, the hydration of these fully hydrated samples was stopped, as described above. XRD analysis showed that there were no clinker minerals remaining in the cement paste samples, demonstrating that fully hydrated PC and PG samples had been obtained. The non-evaporable water contents of these samples were then determined by high-temperature calcination. Finally, the content of non-evaporable water, relative to that in a fully hydrated paste of the same cement, was used as a measurement of the degree of hydration.

### 3 Results and discussion

#### 3.1 Pozzolanic activity of ACG

The specific pozzolanic activity of the ACG present in the ACG-CH-gypsum blend was analyzed. From the DSC, the amount of CH in the ACG not participating in the pozzolanic reaction after 360 d of curing was about 14% (w/w) (Fig. 5). The initial CH content of the blend was 37% (w/w), and therefore the amount of CH consumed by the ACG after 360 d of curing was about 23% (w/w). Since the initial ACG content was 56% (w/w), the result shows that 1 g ACG can consume 0.4 g CH in 360 d in the presence of gypsum and at a water binder ratio of 0.3 while stored in an airtight sealed container at 20  $^{\circ}\text{C}$ .

#### 3.2 Hydration process of cement

##### 3.2.1 Reaction exotherm

Fig. 6 shows the heat evolved by curing PC and

PG as determined by isothermal calorimeter. The dotted lines in Fig. 6 are obtained from PC data multiplied by 70% to calculate an estimated heat evolved from cement clinker hydration in PG.

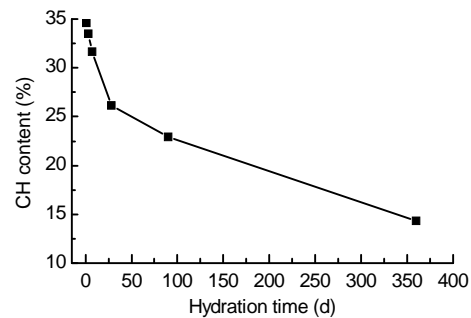


Fig. 5 Calcium hydroxide (CH) content of the activated coal gangue-calcium hydroxide-gypsum blend

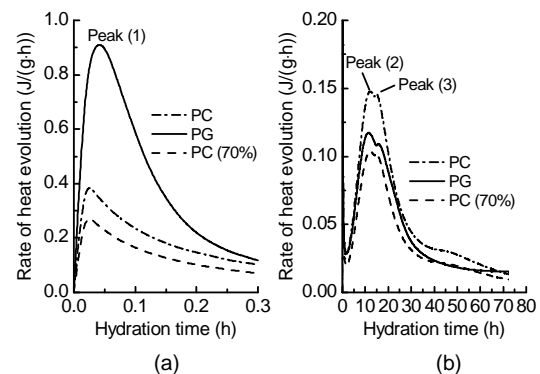


Fig. 6 Rate of heat evolution at 20  $^{\circ}\text{C}$  for Portland cement and the blended sample (a) 0–18 min; (b) 0–72 h

For PC, an initial peak (1) appears at a hydration time of 1 min, with a heat evolution rate of 0.42 J/(g·h), and for PG the initial peak is at 2 min and 0.92 J/(g·h) (Fig. 6a). The main peak (2) of both cements appears at about 12 h, with heat evolution rates of 0.15 and 0.12 J/(g·h), respectively (Fig. 6b). Both cements show a shoulder or more definite peak (3) at about 16 h, with heat evolution rates of 0.14 and 0.11 J/(g·h) (Fig. 6b). The total heats evolved at 72 h were 233 and 197 J/g, respectively.

The heat evolution of the initial peak (1) of PG is more than twice that of PC and more than three times the calculated level (the dotted line). The main peak (2) is below that of PC but above the dotted line. This is due to the dilution effect, which accelerates cement clinker hydration in PG paste. The substitution of ACG for cement increases the water cement ratio and

the contact surface between cement particles and water. This shows that the acceleration effect is more significant in the early period (the initial peak) than in the later period (the main peak and the shoulder peak). The total heat evolution of PG for 72 h is lower than that of PC because the 30% (w/w) ACG is an equal mass replacement for cement, but it is still higher than the 70% scaling of data obtained from PC, which also reveals the dilution effect.

### 3.2.2 Calcium hydroxide (CH) content

The evaluation of the degree of pozzolanic reaction of ACG in the blended cement is based on DSC examination. Fig. 7 shows how the CH content of PC and PG varies with hydration time. The dotted line is obtained from PC data multiplied by 70% to calculate an estimated content of CH produced by cement clinker hydration in PG.

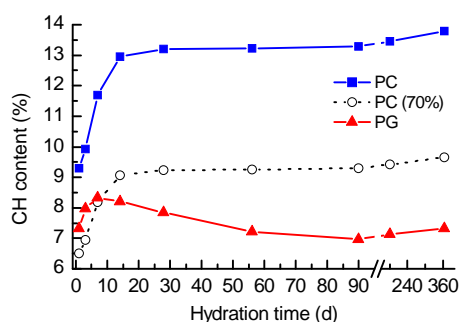


**Fig. 7 Calcium hydroxide (CH) content of Portland cement and the blended sample**

The CH content of PC increases with hydration time. It is above 9% (w/w) at 1 d, about 13% (w/w) at 28 d, and less than 14% (w/w) at 360 d. This shows that the rate of increase in CH content reduces with hydration time particularly after 28 d.

CH in the PG blend is produced mainly by calcium silicate hydration, and is consumed by the pozzolanic reaction of the ACG. The variation in the amount of CH reflects the complex effect of CH production by cement clinker hydration and consumption by pozzolanic reaction. This means that the CH content in the cement paste decreases when the amount of CH consumed is greater than the amount produced. Hence, the degree of hydration of the cement clinker and the degree of reaction of the ACG can be followed by examining the amount of CH present.

For the PG blend, the CH content at 1 d is about 7% (w/w), which is above the dotted line. This means that the dilution effect accelerates the hydration of the cement clinker and hence more CH is produced than that from the equivalent pure cement paste. The CH content increases ( $\geq 8\%$ , w/w) with hydration time up to 7 d. At 14 d, the CH content for the PG blend is lower than that at 7 d and below the dotted line, since the amount of CH consumed by the ACG is greater than that produced by the cement clinker. It can be concluded that the pozzolanic reaction of ACG in blended cement occurs no later than 14 d after the start of curing. Later, the amount of CH consumed by the ACG is always greater than that produced by the cement clinker and the CH content decreases all the way up to a minimum at 90 d. Therefore, the main pozzolanic reaction period of ACG is from 7 to 90 d. After 90 d, the CH content increases gradually because the reactivity of the ACG decreases during this period, and the amount of CH consumed by the pozzolanic reaction is less than that produced by cement clinker hydration. At 360 d, the CH content is about 7% (w/w). From the evaluation of the pozzolanic activity of ACG in the ACG-CH-gypsum blend, it is observed that 1 g ACG can consume 0.4 g CH after 360 d (Section 3.1). Hence, the equal substitution of ACG for 30% (w/w) cement in the blended system will theoretically consume 12% (w/w) CH. The CH content of PG at 360 d is actually about 7% (w/w), plus 12% (w/w) CH theoretically consumed by the ACG, and the CH produced by cement clinker hydration in PG is therefore about 19% (w/w). This is greater than the CH content of about 9% (w/w) evolved after 360 d in the equivalent pure cement paste as the dotted line shows in Fig. 7. Therefore, the pozzolanic reaction of ACG occurs later in the blended cement and accelerates the hydration reaction.

### 3.2.3 Degree of hydration

Fig. 8 shows the degree of hydration of PC and PG plotted against hydration time. Because of the dilution effect in the early stages, and because of the acceleration effect between the cement clinker and the active constituents of ACG in the later stages, the degree of hydration of the PG blend is higher than that of the PC after 1 d. Combined with the information in Fig. 7, the increase in the degree of hydration of the

PG blend before 7 d is mainly due to dilution, and hence more CH is produced. Between 7 and 90 d, the production is mainly due to the acceleration effect between cement clinker hydration and pozzolanic reaction. After 90 d, the difference in degree of hydration between PC and the PG blend gradually becomes constant. This is due to the fading of the pozzolanic reaction of the ACG over time and the dominance of the hydration process in the cement. The constant difference in CH content between PC and PG in Fig. 7 after 90 d is in accordance with the variation in the degree of hydration.

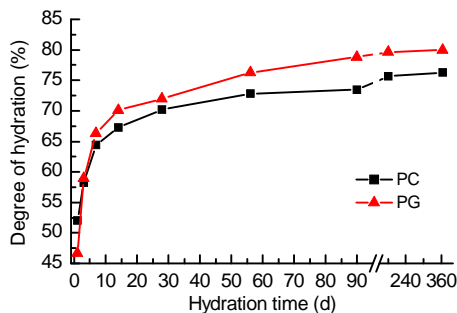


Fig. 8 Degree of hydration of Portland cement and the blended sample

### 3.2.4 Variety of hydrates

Fig. 9 shows the XRD analyses of PC and the PG blend after 360 d of hydration. The chemical and mineral compositions of the materials are significantly different. However, the main active elements of ACG are Si, Al, Ca, and S, which are the same as PC; hence, the main varieties of hydrates found in the PG blend are similar to those found in the PC. The crystal hydrates are portlandite ( $\text{Ca}(\text{OH})_2$ , CH), calcium aluminum oxide hydrate ( $\text{Ca}_3\text{Al}_2\text{O}_6 \cdot x\text{H}_2\text{O}$ , C-A-H), ettringite ( $\text{Ca}_6\text{Al}_2(\text{SO}_4)_3(\text{OH})_{12} \cdot 26\text{H}_2\text{O}$ , AFt), and monosulfate ( $\text{Ca}_4\text{Al}_2\text{SO}_{10} \cdot 12\text{H}_2\text{O}$ , AFm). For the PG blend, the characteristic quartz peaks indicate that it remains as an inert component in the hardened PG paste after 360 d of hydration. The peak intensity of CH is weaker than that of PC since the ACG reacted with CH-the pozzolanic reaction. The characteristic peaks of C-A-H and AFt are more distinct than those of PC, whereas the characteristic peaks of AFm are less distinct. It is perhaps due to the existence of a greater proportion of  $\text{Al}_2\text{O}_3$  and less  $\text{SO}_3$  in the PG

blend than in the PC, meaning that C-A-H and AFt are more easily produced and there is less AFm to be transformed into AFm.

The more distinct diffuse hump from  $20^\circ$  to  $40^\circ$  in the PG blend (Fig. 9) compared with that in the ACG (Fig. 2) indicates the existence of amorphous hydrates-mainly C-S-H gel in the  $\text{CaO-Si}_2\text{O-Al}_2\text{O}_3$  system. Through the calculation of the integrated intensity of background in XRD pattern from  $5^\circ$  to  $75^\circ$ , the C-S-H content can be evaluated semi-quantitatively. The evaluation of the C-S-H content is done as follows:

1. Calculate the integrated intensity of background in XRD patterns of unhydrated cement and hydrated cement pastes. The latter minus the former is the integrated intensity of C-S-H phase in the pastes ( $B$ ).

2. Calculate the integrated intensity of all peaks except the background in XRD patterns of hydrated cement pastes as the integrated intensity of crystal phases in the pastes ( $I$ ).

3. The C-S-H content ( $w_{\text{C-S-H}}$ ) is evaluated as  $w_{\text{C-S-H}} = B/(B+I) \times 100\%$ .

Since there are less cementitious and more inert constituents (such as quartz) in the PG blend, the C-S-H content in the hardened PG paste after 360 d of hydration (about 51%, w/w) is less than that of hardened PC paste (about 56%, w/w). However, the C-S-H content of the PG blend is much more than that of 70% (w/w) PC (about 39%, w/w), being nearer to that of pure PC, due to the pozzolanic reaction in the later hydration period.

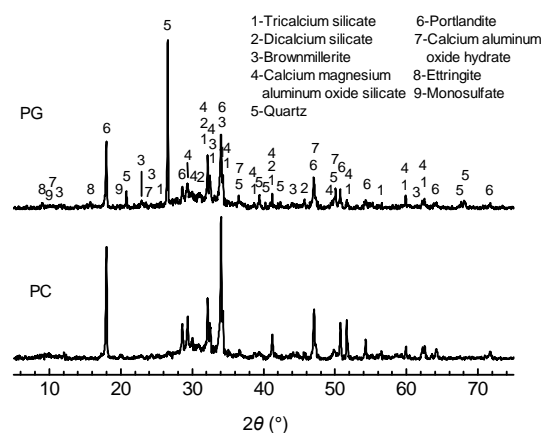


Fig. 9 X-ray diffraction patterns of Portland cement and the blended sample hydrated for 360 d

### 3.3 Compressive strength of hardened cement paste

Fig. 10 shows the compressive strength development of PC and the PG blend in relation to the hydration time. The development of strength is mainly dependent on the degree of hydration: for PC it is clinker hydration and for the PG blend, it is the combination of clinker hydration and the pozzolanic reaction of the ACG. Therefore, the graphs of the strength of the PC and the PG blend versus hydration time provide an insight into the rates of reaction in both types of cement.

The compressive strength of the PC at 3 d is over 50% of that at 360 d; however, after 28 d, the compressive strength development slows down. This is because the rate of cement clinker hydration is fast in the first 3 d, but it slows later (after 28 d). During hydration, the compressive strength of the PG blend is always below that of the PC because the PG blend has less cementitious components and a higher water cement ratio than the PC. However, after 28 d the increase in compressive strength of the PG blend is higher than that of the PC. C-S-H gel is the main contributor to the strength development of cement. For the PG blend, the C-S-H gel comes from the process of cement clinker hydration, as well as from the pozzolanic reaction of the ACG. The main pozzolanic reaction period of ACG is from 7 to 90 d (Section 3.2.2). Up to 28 d, the C-S-H formation, due to the pozzolanic reaction, is slower than formation resulting from cement clinker hydration. However, after 28 d, the continuous increase in compressive strength is mainly due to C-S-H formation by pozzolanic reaction rather than by cement clinker hydration. Although the reactivity of ACG decreases after 90 d (Section 3.2.2), the compressive strength of the PG blend approaches that of the PC (107 MPa), reaching about 97 MPa after 360 d. This confirms that even long-term cement strength is affected by the ACG in a positive way.

Fig. 11 shows compressive strength in relation to the degree of hydration of PC and the PG blend. The relationship can be modeled using an equation in the form  $y=ax^b$ , where  $a$  and  $b$  are constants. At the same degree of hydration, the compressive strength of PC is higher than that of the PG blend. Combined with the results of Sections 3.2.3 and 3.2.4, the degree of hydration of the PG blend at 360 d is higher than that of

the PC, but the C-S-H content is lower. In other words, the PG blend produces less C-S-H than the PC at the same degree of hydration, resulting in a lower compressive strength.

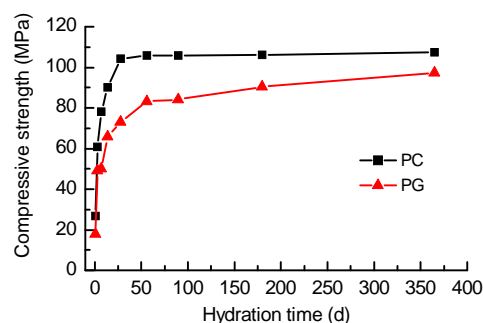


Fig. 10 Compressive strength development of Portland cement and the blended sample

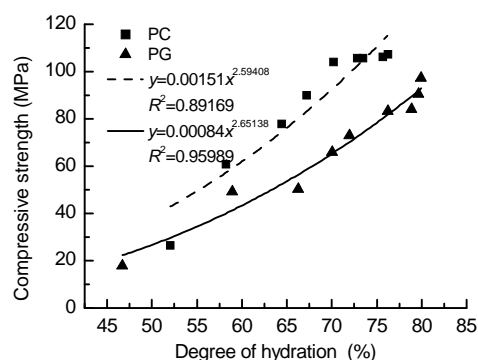


Fig. 11 Compressive strength in relation to the degree of hydration

## 4 Conclusions

Based on the above investigation, the following conclusions can be drawn:

The reactivity of ACG comes from amorphous  $\text{SiO}_2$  and  $\text{Al}_2\text{O}_3$  present as metakaolin. The metakaolin exhibits pozzolanic activity when in an ACG-CH-gypsum blend or an ACG-Portland cement blend.

In blended cement, the dilution effect of ACG accelerates cement clinker hydration, which is more significant early in the cure process, rather than later. In addition, the pozzolanic reaction of ACG occurs mainly during the first 7 to 90 d, consuming CH and accelerating the hydration of the cement clinker. Hence, the hydration degree of blended cement is higher than that of pure Portland cement when cured for the same amount of time.

The main varieties of hydrate in the blended cement are similar to those present in pure Portland cement, but the quantity of C-S-H is quite different, which results in the difference in compressive strength development between the two cements.

The compressive strength of blended cement eventually approaches that of pure Portland cement even when ACG is substituted for Portland cement at 30% (w/w). ACG can be treated as one of a number of potential SCMs since it does little harm to the long-term compressive strength of hardened cement paste and it reduces the amount of clinker used in the blended cement.

## References

- Feng, B., 2000. Study on coal-refuse activity. *Shanghai Environmental Science*, **19**(7):349-351, 353 (in Chinese).
- Kakali, G., Perraki, T., Tsvilis, S., Badogiannis, E., 2001. Thermal treatment of kaolin: the effect of mineralogy on the pozzolanic activity. *Applied Clay Science*, **20**(1-2): 73-80. [doi:10.1016/S0169-1317(01)00040-0]
- Li, C., Wan, J.H., Sun, H.H., Li, L.T., 2010. Investigation on the activation of coal gangue by a new compound method. *Journal of Hazardous Materials*, **179**(1-3):515-520. [doi:10.1016/j.jharmat.2010.03.033]
- Li, D.X., Song, X.Y., Gong, C.C., Pan, Z.H., 2006. Research on cementitious behavior and mechanism of pozzolanic cement with coal gangue. *Cement and Concrete Research*, **36**(9):1752-1759. [doi:10.1016/j.cemconres.2004.11.004]
- Lippmaa, E., Mägi, M., Samoson, A., Engelhardt, G., Grimmer, A.R., 1980. Structural studies of silicates by solid-state high-resolution <sup>29</sup>Si NMR. *Journal of the America Chemical Society*, **102**(15):4889-4893. [doi:10.1021/ja00535a008]
- Liu, X.P., Wang, P.M., 2008. Interface structure of Portland coal gangue blended cement. *Journal of the Chinese Ceramic Society*, **36**(1):104-111 (in Chinese).
- Palomo, A., Blanco-Varela, M.T., Granizo, M.L., Puertas, F., Vazquez, T., Grutzeck, M.W., 1999. Chemical stability of cementitious materials based on metakaolin. *Cement and Concrete Research*, **29**(7):997-1004. [doi:10.1016/S0008-8846(99)00074-5]
- Rojas, M.F., Sánchez de Rojas, M.I., 2005. Influence of metastable hydrated phases on the pore size distribution and degree of hydration of MK-blended cements cured at 60 °C. *Cement and Concrete Research*, **35**(7):1292-1298. [doi:10.1016/j.cemconres.2004.10.038]
- Shigemoto, N., Sugiyama, S., Hayashi, H., Miyaura, K., 1995. Characterization of Na-X, Na-A, and coal fly ash zeolites and their amorphous precursors by IR, MAS NMR and XPS. *Journal of Materials Science*, **30**(22):5777-5783. [doi:10.1007/BF00356720]
- Shvarzman, A., Kovler, K., Grader, G.S., Shter, G.E., 2003. The effect of dehydroxylation/amorphization degree on pozzolanic activity of kaolinite. *Cement and Concrete Research*, **33**(3):405-416. [doi:10.1016-S0008-8846(02)00975-4]
- Singh, P.S., Trigg, M., Burgar, I., Bastow, T., 2005. Geopolymer formation processes at room temperature studied by <sup>29</sup>Si and <sup>27</sup>Al MAS-NMR. *Material Science and Engineering A*, **396**(1-2):392-402. [doi:10.1016/j.msea.2005.02.002]
- Wang, P.M., Liu, X.P., 2011. Effect of temperature on the hydration process and strength development in blends of Portland cement and activated coal gangue or fly ash. *Journal of Zhejiang University-SCIENCE A (Applied Physics & Engineering)*, **12**(2):162-170. [doi:10.1631/jzus.A1000385]
- Wang, P.M., Liu, X.P., Hu, S.G., Nü, L.N., Ma, B.G., 2007. Hydration models of Portland coal gangue cement and Portland fly ash cement. *Journal of the Chinese Ceramic Society*, **35**(S1):180-186 (in Chinese).
- Wei, Q.W., Gao, W.Y., Sui, X.G., 2010. Synthesis of low-temperature, fast, single-firing body for porcelain stoneware tiles with coal gangue. *Waste Management and Research*, **28**(10):944-950. [doi:10.1177/0734242X09351734]
- Xie, X.W., 2009. Comprehensive utilization of coal gangue. *Shanghai Environmental Science*, **22**(S1):121-123 (in Chinese).
- Zhang, J.X., Sun, H.H., Sun, Y.M., Zhang, N., 2010. Corrosion behavior of steel rebar in coal gangue-based mortars. *Journal of Zhejiang University-SCIENCE A (Applied Physics & Engineering)*, **11**(5):382-388. [doi:10.1631/jzus.A0900443]
- Zibouche, F., Kerdjoudj, H., Lacaille, J.B.d.d., Damme, H.V., 2009. Geopolymers from Algerian metakaolin. Influence of secondary minerals. *Applied Clay Science*, **43**(3-4):453-458. [doi:10.1016/j.clay.2008.11.001]